Calculation of the ELF in the excited state with single determinant methods

Andrea Echeverri,[1] Miguel Gallegos,[2] Tatiana Gómez,[3] Ángel Martín Pendás,[2] and Carlos Cárdenas[1,4]
[1)]*Departamento de Física, Facultad de Ciencias, Universidad de Chile, Casilla 653, Santiago, Chile.*
[2)]*Depto. Química Física y Analítica. Universidad de Oviedo. 33006 Oviedo, Spain.*
[3)]*Theoretical and Computational Chemistry Center, Institute of Applied Chemical Sciences, Faculty of Engineering, Universidad Autonoma de Chile, El Llano Subercaceaux 2801, Santiago, Chile*
[4)]*Centro para el Desarrollo de la Nanociencia y la Nanotecnología (CEDENNA), Avda. Ecuador 3493, Santiago 9170124, Chile.*

(*Electronic mail: cardena@uchile.cl)

(*Electronic mail: ampendas@uniovi.es)

(Dated: 18 January 2023)

Since its first definition, back in 1990, the Electron Localization Function (ELF) has settled as one of the most commonly employed techniques to characterize the nature of the chemical bond in real space. Although most of the work using the ELF has been focused on the study of ground-state chemical reactivity, a growing interest has blossomed to apply these techniques to the nearly unexplored realm of excited states and photochemistry. Since accurate excited electronic states usually require to account appropriately for electron correlation, the standard single-determinant ELF formulation cannot be blindly applied to them, and it is necessary to turn to correlated ELF descriptions based on the two-particle density matrix (2-PDM). The latter require costly wavefunction approaches, unaffordable for most of the systems of current photochemical interest. Here, we compare exact, 2-PDM-based ELF results with those of approximate 2-PDM reconstructions taken from Reduced Density Matrix Functional Theory (RDMFT). Our approach is put to the test in a wide variety of representative scenarios, such as those provided by the lowest-lying excited electronic states of simple diatomic and polyatomic molecules. Altogether, our results suggest that even approximate 2-PDMs are able to accurately reproduce, on a general basis, the topological and statistical features of the ELF scalar field, paving the way toward the application of cost-effective methodologies, such as TD-HF or TD-DFT, in the accurate description of the chemical bonding in excited states of photochemical relevance.

I. INTRODUCTION

The molecular structure hypothesis, supplemented with the chemical bond noumenon, constitutes one of the foundational paradigms of the Chemical Sciences. In modern parlance, matter is typically described in terms of a collection of interacting particles held together by either classical chemical bonds or by considerably weaker non-covalent interactions (NCI), while chemical reactivity is understood as the evolution and transformation of their spatial arrangement and connectivity. In a first approximation, chemists simply evolve 3D-embedded undirected graphs, so that if the building blocks of matter, the atoms, are identified with the vertices of the graphs, so are the basic entities of chemical structure be associated with the edges, or bonds. It is astonishing how experimental evidence led chemists to such a topological picture well before the discovery of the electron[1], the elucidation of the basic structure of atoms[2], or the first quantum mechanical rationalization of their stability.[3] Within a few decades, the cubical atom of paired electrons proposed by G. N. Lewis[4] and the Valence Shell Electron Pair Repulsion (VSEPR) model of Gillespie[5] resulted in a division of the molecular space (R^3) into bonding/lone pair domains that exclude the presence of other pairs due to the Pauli exclusion principle. With a few exceptions,[6] these simple principles are extremely successful at explaining the structure and bonding of ground state molecules, to the point that they can be easily taught to fresh students. From the standpoint of Physics, and under the Born-Oppenheimer approximation[7], the structure of a molecule arises from the Coulombic interaction among its electrons in the electric field induced by clamped nuclei. Although electronic energies can be accurately estimated from approximate solutions of the Schrödinger equation, the large dimensionality and complexity of wavefunctions, which exist in a H^N Hilbert space, make it extremely difficult to transition from a physical description to the chemical objects just described. Furthermore, the chemical bond lacks a properly defined Dirac operator, and it is thus not an observable in quantum mechanics. Despite these inconveniences, the field of Quantum Chemical Topology (QCT)[8] has been very successful in linking quantum mechanics with a canonical interpretation of the chemical bond and molecular structure. QCT focuses on the topological analysis of scalar fields (built from wavefunctions) in R^3. For instance, the topological analysis of the electron density, $\rho(\mathbf{r})$, which constitutes the basis of the Quantum Theory of Atoms in Molecules (QTAIM)[9], provides a standalone definition of atoms in molecules and their interconnections. A complementary partitioning of the space in terms of localized electron pairs can be conveniently achieved by means of the Electron Localization Function (ELF)[10–15]. In this way, a chemically appealing representation and analysis of the electronic structure of molecules becomes available, allowing for an intuitive rationalization of computed wavefunctions in terms of the classical Lewis and VSEPR models

of the covalent or ionic bonds together with the remaining lone electron pairs.

The ELF was introduced in 1990 by Becke and Edgecombe, initially for single-determinant Hartree-Fock (HF) wavefunctions.[10] Later, Savin showed that this original operational definition also held in ground state density functional theory (DFT).[11] Since then, the ELF has been shown to admit several complementary interpretations,[16–18] among which two stand out for our purposes.

According to the first one, large ELF values indicate regions in space where the probability of finding a localized pair of electrons is particularly high. This result arises naturally from the original definition of the ELF, $\eta(\mathbf{r})$,

$$\eta(\mathbf{r}) = \left(1 + (\frac{D(\mathbf{r})}{D_0(\mathbf{r})})^2\right)^{-1}, \tag{1}$$

Here, $D(\mathbf{r})$ is the curvature of the conditional probability density, $P^{\sigma\sigma}(\mathbf{r})$, to find an electron of spin σ at a spherically averaged distance s around a point $\mathbf{r}$ where another same-spin electron is known to lie. Given that $P^{\sigma\sigma}(\mathbf{r},\mathbf{s}) = \pi^{\sigma\sigma}(\mathbf{r},\mathbf{s})/\rho^{\sigma}(\mathbf{r})$, where $\pi^{\sigma\sigma}$ and ρ^{σ} are the same-spin two-particle density matrix (2-PDM) and the σ spin component of the electron density, respectively,

$$D(\mathbf{r}) = \frac{1}{2}\nabla_s^2 P^{\sigma\sigma}(\mathbf{r},\mathbf{r}+\mathbf{s})\Big|_{\mathbf{s}=\mathbf{0}} = \left(\sum_i^{\sigma} |\nabla\psi_i(\mathbf{r})|^2 - \frac{1}{4}\frac{|\nabla\rho^{\sigma}(\mathbf{r})|^2}{\rho^{\sigma}(\mathbf{r})}\right) \tag{2}$$

where the right-hand side shows an expansion of D in terms of the occupied molecular orbitals (with spin σ) of a HF wavefunction, ψ_i. D_0 is the value of D as computed for a non-interacting homogeneous electron gas, and makes ELF dimensionless and density independent. From these expressions, it becomes evident that the smaller the probability of finding two same-spin electrons in a region becomes, the more localized the reference electron is.

A second relevant interpretation of ELF uses the kinetic energy of the electrons, and starts by identifying the first term of $D(\mathbf{r})$ as half the positive-definite kinetic energy density of a system with mean-field-interacting electrons, while noticing that the second is half the kinetic energy density of a system of bosons with the same density. D is thus measuring the excess kinetic energy density of a ferminonic system with respect to a bosonic one as a result of Pauli's principle,[11,13] so that large D values are to be associated with regions where electrons will not localize and vice versa. This kinetic interpretation is crucial in density functional theory (DFT), as it allows to use Kohn-Sham (KS) orbitals in Eq. 2 even though the original derivation held only for an HF wavefunction. We note in passing that the ELF also admits another interpretation in terms of the monoelectronic character of the wavefunction, since for a single-electron system $D(\mathbf{r})$ is null and the ELF is maximal ($\eta = 1$) at all points. In a many-electron scenario the ELF peaks locally in regions where the wavefunction has a strong monoelectronic character. This feature is especially useful to characterize Rydberg states, in which an electron is weakly bound to the molecular frame. The large value of ELF in monoelectronic regions has been used, for instance, in the development of the SCAN functional by Perdew.[19]

No matter which of the aforementioned interpretations is used, the role that QCT descriptors, such as the ELF, have played in the study of chemical bonding and the electronic structure of molecules and solids is undeniable. However, most of the work done in the context of QCT has been devoted to the characterization of ground-state systems, and only moderate attention has emerged in recent years on extending these efforts to the photochemistry realm, with the aim of shining light on the changes undergone by chemical bonds upon electronic excitation[20–34]. The importance of this extension is further motivated by the overwhelming abundance of new phenomena taking place in excited states such as in the photodissociation[35] and photoisomerization[36] of a large number of molecules. Additionally, electronic excitation allows for a wide range of ground-state-forbidden chemical transformations to take place, such as cyclizations[37], isomerizations[38], proton transfer reactions[39] or even electron rearrangements,[40] to name just a few possibilities that are opening the way to a whole new spectrum of chemical reactions. Also, the limited vibrational phenomena found in ground states are typically replaced by a much richer adiabatic and non-adiabatic dynamics in excited states. As a result of this variety, photochemistry is nowadays an exciting field with technologically important outcomes that range from solar cell manufacturing[41] to surface chemistry,[42] chemical sensing[43], or self-cleaning materials[44] applications. Recently, excited state chemistry has even been coupled to quantum electrodynamics (QED) when electrons are explicitly coupled to the photon field.[45] Taking all of the above into account, it becomes evident that the development of theoretical tools as well as efficient algorithms to characterize the chemical bond in excited states is of utmost importance.

At first glance, one might be tempted to use the original formulation of the ELF to study this and related chemical phenomena. Unfortunately, and despite its intuitive and rational derivation, the single-determinant origin of the 2-PDM appearing in Eq. 2 prevents electronic correlation effects from being effectively taken into account. This is particularly inconvenient, as electron correlation is known to play a fundamental role in the understanding of a rich variety of chemical phenomena , particularly in excited states.[46,47] In this paper, we examine to what extent the introduction of correlation effects through the explicit consideration of the 2-PDM affects the ELF, paying particular attention to the accuracy of approximate reconstructions of the two-particle density that can be used in the case of DFT derived wavefunctions. Our results show that it is feasible to get accurate descriptions of the chemical bonding in excited states from these approximate ELF expressions, that are put to the test in a wide variety of scenarios, in a number of test-bed excited electronic states of simple well-known molecules of different size, such as water or benzene. The paper is organized as follows: first, a brief overview of the theoretical background of the ELF kernel along with the reconstruction of 2-PDM in terms on natural orbitals and occupation numbers is presented. Then, in a set

of different molecules and excited states we assess the effect of including electron correlation in the ELF calculation using a CASSCF wavefunctions and several reconstructions of the 2-PDM coming from TD-DFT and TD-HF calculations. The final section gathers the conclusions that can be drawn from our work.

II. THEORETICAL METHODS

Research on correlation effects in ELF is scarce and requires avoiding the use of single-determinant expansions and, in some cases, preventing normalization to the homogeneous electron gas (HEG). For instance, Dobson and Silvi[48–50] derived the ELF from local integration of the conditional pair density. More recently, Matito et al.[51] showed that Dobson's and Savin's results were in fact equivalent and that the ELF in a correlated scenario could be obtained from

$$\frac{D(\mathbf{r})}{D^{HEG}(\mathbf{r})} = \frac{\nabla_s^2 \pi^{\beta\beta}(\mathbf{r},\mathbf{r}+\mathbf{s})|_{s=0} + \nabla_s^2 \pi^{\alpha\alpha}(\mathbf{r},\mathbf{r}+\mathbf{s})|_{s=0}}{2c_F \rho^{8/3}(\mathbf{r})}. \quad (3)$$

The above expression is obviously invariant under orbital transformations, independent on the electronic state of the system and applicable to any wavefunction, either single- or multi-determinant. In this way, Eq. 3 can be used for both ground and excited states, including electron correlation or not. Under this more general approach, all that is necessary is an expression for the 2-PDM, $\pi^{\sigma\sigma}$, of the electronic state under investigation. As an example, one can reconstruct an approximate 2-PDM from a time-dependent density functional theory (TD-DFT) calculation in terms of the natural orbitals (NO), $\left\{\phi_i^{(k)}\right\}$, and occupations numbers, n_i, of the corresponding TD-DFT density matrix, as:

$$\pi^{\sigma\sigma}_{(k)}(\vec{r}_1,\vec{r}_2) = \sum_{i\in\sigma}\sum_{j\in\sigma} n_i n_j \left(\phi_i^{(k*)}(\vec{r}_1)\phi_j^{(k*)}(\vec{r}_2)\phi_i^{(k)}(\vec{r}_1)\phi_j^{(k)}(\vec{r}_2) - \phi_i^{(k*)}(\vec{r}_1)\phi_j^{(k*)}(\vec{r}_2)\phi_j^{(k)}(\vec{r}_1)\phi_i^{(k)}(\vec{r}_2)\right). \quad (4)$$

Indeed, using such a simple procedure, some of us have successfully studied the proton transfer of salicylidene methylamine in the excited state.[31] By replacing Eq. 4 in Eq. 3 one arrives to the uncorrelated ELF for excited states proposed by Maulen et al.[31]

$$\eta^{(k)}(\vec{r}) = \frac{1}{1+\left(\frac{\sum_i^\sigma n_i |\nabla\phi_i^{(k)}(\vec{r})|^2 - \frac{1}{4}\frac{|\nabla\rho^{\sigma,(k)}(\vec{r})|^2}{\rho^{\sigma,(k)}(\vec{r})}}{\frac{3}{5}6\pi^2\rho^{\sigma,(k)}(\vec{r})^{5/3}}\right)^2}, \quad (5)$$

which has been used by Guerra et al.[34] to reinterpret archetypal chemical reactions in excited states and by some of us to guide the rational design of bio-markers[52]. The reconstruction of the 2-PDM in terms of NOs to compute the ELF in the ground state has been attempted before. Matito et al.[53] showed that an HF-like reconstruction (Eq. 4) is exceptionally accurate at recovering the correlated topology of ELF in molecules with low to medium static correlation. Contrarily, statistical properties depending on the 2-PDM, such as the fluctuation of the ELF basin populations or the inter-basin ELF covariances, seemed to be particularly more sensitive to the quality of 2-PDM.[53]

Correlation effects are expected to be more important in excited than in ground states. This becomes especially pronounced in the case of high-energy excitations, where the energy gap between neighboring states decreases with the excitation energy, thus increasing the impact of static correlation. In the conventional excited state calculations framework, static correlation is often accounted for via multireference methods, such as CASSCF, from which the 2-PDM can be extracted exactly. Unfortunately, these are computationally demanding and cannot be routinely employed to study the complex systems of state-of-the-art chemical research, such as dyes. Instead, a reasonably accurate treatment of the excited states of systems of medium to large size can be achieved with the aid of Time-Dependent Density Functional Theory (TD-DFT). Actually, TD-DFT has settled as one of the most commonly applied methodologies to study the photochemistry of molecules with up to hundreds of atoms. Unfortunately, TD-DFT, as DFT itself, lacks any true 2-PDM, raising the need of approximately reconstructing it in terms of the 1-PDM NOs and their corresponding occupation numbers. Albeit this not possible in an exact way, quantum mechanics establishes certain rules that must be fulfilled and that help us in such an enterprise. Some examples include the N-representability[54] condition, the so-called sum rule, (Eq. 9) as well as some characteristic (a)symmetries that ensure the physical rigor of the 2-PDM.[55,56] Relying on these, the Reduced Density Matrix Functional theory (RDMFT) has provided over the years a wealth of approximate reconstructions of the 2-PDM. RDMFT is grounded on Gilbert's theorem,[57] which establishes, in analogy to the Hohenberg-Kohn theorem[54], that there is a one to one mapping between the first order reduced density matrix, 1-RDM, and the ground state energy and wavefunction.

Most of the 2-PDM reconstruction models that have been proposed within RDMT can be put in a common framework if we write the 2-PDM in the basis of NO products $\phi_i^{(k)*}(\vec{r}_1)\phi_j^{(k)*}(\vec{r}_2)\phi_k^{(k)}(\vec{r}_1)\phi_l^{(k)}(\vec{r}_2)$. In this (particle-hole) ba-

sis, the HF reconstruction of the 2-PDM is simply

$$\Pi_{ijkl} = n_i n_j \delta_{ik} \delta_{jl} - n_i n_j \delta_{il} \delta_{jk}, \tag{6}$$

where the first term is the "direct" part while the second, or "exchange" one, comes from antisymmetry. Taking this into account, more general expressions that will capture Coulomb correlation effects are usually written as

$$\Pi_{ijkl} = f(n_i, n_j) \delta_{ik} \delta_{jl} - g(n_i, n_j) \delta_{il} \delta_{jk}, \tag{7}$$

where $f(n_i^\sigma, n_j^\sigma)$ and $g(n_i^\sigma, n_j^\sigma)$ are functions of the previous occupation numbers, which are usually chosen so as to incorporate as much electron correlation as possible at the expense of lifting some of the exact conditions that the 2-PDM must fulfill. In this regard, it has been argued [REF] that preserving both the Pauli principle and the sum rules of the 2-PDM are absolute musts when it comes to computing and analyzing the topological features of the ELF field. Thus, we should ensure, first, that

$$\pi_{(k)}^{\sigma\sigma}(\vec{r}_1, \vec{r}_1) = 0, \tag{8}$$

so that the local fermionic kinetic energy excess sensed by the ELF is accurately modeled. However, as we shall see, violation of this condition has no major consequences in practice. Similarly, the sum rule ensuring that the 2-PDM integrates to the exact number of same-spin electron pairs

$$\int\int \pi_{(k)}^{\sigma\sigma}(\vec{r}_1, \vec{r}_2) d\vec{r}_1 d\vec{r}_2 = N^\sigma (N^\sigma - 1), \tag{9}$$

is expected to play a significant role in the topological analysis of any gradient field, since it behaves as a scale factor. For instance, the covariance between the population of two non-overlapping basins Ω_1 and Ω_2 involves integrations of the 2-PDM,

$$cov(\Omega_1, \Omega_2) = \int_{\Omega_1}\int_{\Omega_2} (\pi_{(k)}(\vec{r}_1, \vec{r}_2) - \rho_k(\vec{r}_1)\rho_k(\vec{r}_2)) d\vec{r}_1 d\vec{r}_2, \tag{10}$$

and violation of the sum rule leads to improperly behaving covariances.

Either following or not the aforementioned rules, a lot of work has been devoted over the years to derive suitable functional forms for the kernel of Eq. 7. In this context, several notoriously successful and well-known approaches can be highlighted including the Buijse-Baerends approach(BB)[58,59]; the Goedecker-Umrigar (GU)[60] and BBC2[61] functionals, developed to correct for the self-interaction and overbinding errors inherent to the BB functional; the Csanyi-Arias (CA)[62] and Csanyi-Goedecker-Arias (CGA)[63] functionals, based on tensor product expansions of the 2-PDM; or the empirical Marques-Lathiotakis (ML)[64] and Marques-Lathiotakis-self-interaction-corrected (MLSIC)[64] functionals, written as Pade approximants, to name a few. Explicit expressions of the terms $f(n_i, n_j)$ and $g(n_i, n_j)$ (Eq. 7) for these functionals can be found in Table I. Further details can be found in Section F of the SI.

III. COMPUTATIONAL DETAILS

All calculations were performed in the gas phase without any relativistic corrections, at different levels of theory. Molecular geometries were optimized in the ground state at the DFT level of theory, with the range-separated ω-B97XD functional[65] in combination with the def2-TZVP basis set[66]. Such a range-separated functional, including long-range dispersion corrections, was selected on the basis of its suitability for calculating electronic excitations with TD-DFT. Geometry optimizations were performed with the aid of the Gaussian16[67] quantum chemistry package. Moreover, all the stationary points found were verified to be true minima on their potential energy surfaces through conventional harmonic calculations. ELF calculations in the excited states were done with an in-house modified version of the TopMod code[68] that allows reading both NOs as well as 2-PDMs. For CASSCF wavefunctions, the 2-PDM is built from the CI expansion in the basis of canonical molecular orbitals[55] and the ELF is computed with Eq 3. In TD-DFT there is no wavefunction of the excited state but only its 1-RDM. Once the 1-RDM is transformed into its NO's representation through diagonalization, Eq. 7 is used to reconstruct the 2-PDM with all the functionals described in Table I. Similarly to CASSCF, Eq 3 is used to compute the TD-DFT ELF. It is very important to make it clear that, given a 2-PDM reconstruction, Eqs. 3 and 5 are not equivalent. Instead, they become only coincident in the particular case of and HF reconstruction. CASSCF's wavefunctions of excited states were computed employing an even state-average optimization of orbitals. Namely, when n electronic states with adequate symmetry contribute to the state they were given equal $1/n$ weights. Two types of CASSCF calculations were performed for each excited state: one with the smallest active space needed to represent their wavefunction as observed in TD-DFT and another in which the active space was sufficiently enlarged so as to account for some dynamic correlation. It is important to clarify here that it is not our intention to calculate excited states with extreme precision but to investigate how adequate the 2-PDM reconstructions used to calculate the ELF are under the TD-DFT formalism. For this, it is necessary to ensure that the CASSCF wavefunction corresponds to the states (excitations) actually found in TD-DFT. In summary, given an excited state calculated with TD-DFT, we want to know how much error is made in calculating the ELF from a 2-PDM reconstruction. When large basis sets are used in TD-DFT, it is usual for the natural orbitals corresponding to the highest KS orbitals to have slightly negative occupation numbers (ON). Indeed, Gordon et al.[69] have noted that the occurrence of such negative ON is indicative of the need for a multireference treatment. A decision must then be made as to what to do with them when computing the ELF from 2-PDM reconstructions. One option is to ignore those orbitals completely. Another is to take the absolute value of their very small occupancies. We have examined both possibilities and found that the first option is the one that brings the TD-DFT results closest to the CASSCF benchmarks (see section B in SI). Therefore, in all our results, the first strategy has been adopted.

Approximation	Constrains			
	$f(n_i,n_j)$	$g(n_i,n_j)$	Antisymmetry	Sum Rule
HF	$n_i n_j$	$n_i n_j$	✓	×
BB	$n_i n_j$	$\sqrt{n_i n_j}$	×	✓
BBC2	$n_i n_j$	$\begin{cases} n_i n_j \; j \neq i \; and \; SOcc. \\ -\sqrt{n_i n_j} \; j \neq i \; and \; WOcc \\ \sqrt{n_i n_j} \; otherwise \end{cases}$	×	✓
GU	$n_i n_j(1-\delta_{ij})$	$\sqrt{n_i n_j}(1-\delta_{ij})$	×	×
CGA	$n_i n_j$	$1/2(n_i n_j + \sqrt{n_i(2-n_j)n_j(2-n_j)})$	×	×
ML	$n_i n_j$	$n_i n_j * \frac{a+bn_i n_j}{1+cn_i n_j}$	×	×
MLSIC	$n_i n_j(1-\delta_{ij})$	$n_i n_j * \frac{a+bn_i n_j}{1+cn_i n_j}(1-\delta_{ij})$	×	×

TABLE I. Summary of the pair density reconstructions used in this work. f and g correspond to the functions in Eq 7. The last two columns indicate whether or not the reconstruction strictly preserves the antisymmetry condition and the sum rule.SOcc and WOcc refers to strongly ($\phi_i, i \leq N/2$) and weakly ($\phi_j, j > N/2$) occupied naturals orbitals, respectively.

IV. RESULTS AND DISCUSSION

As the main purpose of this work is to explore the reliability of the computation of the ELF in excited states with methods lacking exact 2-PDM matrices, we have selected a set of molecules and electronic states that are prone to undergo significant changes in their bonding pattern upon excitation. We will thus study the archetypal molecules of hydrogen fluoride (HF), water (H_2O), and benzene (C_6H_6) in their first or second lowest-lying excited states. All these systems have been widely covered in both traditional and recent literature and are small enough to be adequately computed at low and high levels of theory.

Table II summarizes some basic data about the excitations considered in this work. As it can be seen, most lie close to the ionization threshold and, with the exception of benzene, are expected to have a least partial diffuse (Rydberg-like) character.

Molecule	State	E^{exc} (eV)	E^{ion} (eV)	Symmetry	Transition
HF (vert.)	1	9.56	16.03±0.04	$X^1\Sigma^+ \rightarrow A^1\Pi^+$	[H→L]
HF	2	14.97	16.03±0.04	$X^1\Sigma^+ \rightarrow B^1\Sigma^+$	[H-1→L]
HF (adiab.)	2	15.12	16.03±0.04	$X^1\Sigma^+ \rightarrow B^1\Sigma^+$	[H-1→L]
H_2O	1	7.34	12.62±0.00	$^1A_1 \rightarrow {}^1B_1$	[H→L]
C_6H_6	1	5.09	9.24±0.00	$^1A_{1g} \rightarrow {}^1B_{2u}$	[H→L]

TABLE II. Lowest lying excited states of the HF, H_2O, and C_6H_6 molecules studied in this work. Both the CASSCF estimated excitation, E^{exc}, and the experimentally determined ionization, E^{ion}, energies are reported in eV. Term symbols/symmetry of the ground and excited states as well as Kohn-Sham orbitals involved in the transitions are also shown. Experimental data was taken from the literature[70]. The labels H and L are used to refer to the HOMO and LUMO frontier orbitals, respectively. In HF, both the vertical (Franck-Condon) and adiabatic excitations are shown.

A. Hydrogen Fluoride

The $X^1\Sigma^+$ ground state of HF is a singlet dominated by the $(\sigma_{2s})^2(\sigma_{2p})^2(\pi_{2p})^2(\pi_{2p})^2$ valence MOs configuration. On the other hand, the $A^1\Pi^+$ first excited state is a 2-fold spatially degenerate state arising from a $\pi_{2p} \rightarrow \sigma^*_{2p}$ single-electron promotion. Our two CASSCF excitation energies, obtained with (4,3) and (4,6) spaces are 8.57 and 9.64 eV, respectively, lying reasonably close to the experimentally reported value of 10.35 eV[71]. Similar results are obtained with the TD-DFT and TD-HF approaches, with excitation energies of 10.47 and 11.86 eV, respectively. Moreover, in TD-DFT the single-electron transition that contributes the most to the excited state is $\pi_{2p} \rightarrow \sigma^*_{2p}$, as expected. The same is true for TD-HF, although a small contribution from the $\pi_{2p} \rightarrow \sigma^*_{2s}$ promotion is also observed in this case. The $A^1\Pi^+$ dissociates to the ground state $F(^2P) + H(^2S)$.

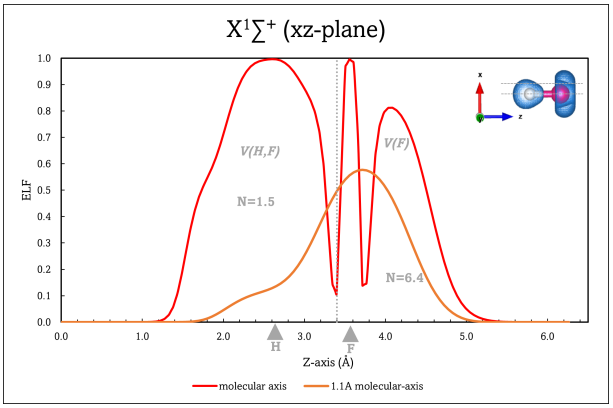

FIG. 1. Profile of the electron localization function (ELF) on the internuclear axis (red), and 1.1Å above of the internuclear axis (orange) in hydrogen fluoride molecule computed with ω-b97xd/def2tzvp in the ground state ($X^1\Sigma^+$). The inset shows the line along which the ELF has been plot and a $ELF = 0.83$ isosurface. F and H are depicted as red and light-gray points in the inset. Positions of F and H are marked with light-gray triangle next to the position axis. Vertical dashed lines indicate the position of basins separatrix.

In order to understand correctly the ELF changes underlying the $X^1\Sigma^+ \rightarrow A^1\Pi^+$ excitation, it is convenient to discuss first the basic features of the ELF field in the ground state. It shows three basins: an F core ($C(F)$) with a population approximately equal to 2 electrons, a valence basin of the F atom ($V(F)$), with 6.4 electrons, and an additional basin attributed to the H-F bond ($V(H,F)$), that bears a total of 1.5 electrons (See Figure 1). These last two basins roughly reconstruct the 8 valence shell electrons of the system. The ELF picture thus corresponds to what is expected for a high polarity molecule, arising from the large electronegativity difference between its constituting atoms.

In the Franck-Condon (FC) $A^1\Pi^+$ state, the ELF exhibits an additional valence basin which was absent in the corresponding basal state (See Figure 2). As we will see, this newly formed basin can be attributed to a fuzzy valence of the H atom which emerges in response to the electron promotion.

Furthermore, although the C(F) basin remains nearly unmodified, the electronic excitation promotes significant changes in the topology and electron count of the remaining ELF valence basins- For instance, whereas the population of the V(F) barely changes, the V(H,F) bond basin undergoes a noticeable decrease in its population in favor of the newly formed hydrogen "valence" basin V(H). Globally, the image of the bond pattern provided by the ELF in the FC geometry of the $A^1\Pi^+$ state corresponds to a weakening of the H-F bond coupled to a concomitant localization of a Rydberg electron close to the hydrogen atom. This is consistent with previous studies which have attributed a strong Rydberg character[71–74] to this state. As mentioned in the introduction, the ELF is particularly useful to uncover monoelectronic regions of the wavefunction. In this and similar scenarios we find an electron weakly bound to the molecule, although strongly correlated with it.

After discussing the general changes induced in the ELF upon the excitation of the system, it is worth exploring how these results change with the level of theory and the accuracy in the reconstruction of the approximate 2-PDM. For such a purpose, one can take a look at Fig. 2 showing the evolution of the ELF scalar field along the main molecular axis. One can see that in the neighborhood of the F atom, the ELF calculated with all the RDMFT reconstructions is quite similar and lies between the results afforded by both CASSCF calculations, used as a golden standard in this work. Instead, the main differences between the TD-DFT and CAS methodologies seem to be found in the vicinity of the separatrix between the V(H,F) and V(H) basins as well as in the V(H) basin, for which any of the RDMFT approaches tend to underestimate the ELF. We note in passing that a large value of the ELF in the separatrix of two basins leads to less defined critical points of the scalar field, something which is commonly referred to as a less persistent topology[75,76]. Chemically, this can be interpreted as a decrease in the electronic localization of the system (i.e., these maxima are less "significant" to identify localization regions). This is, moreover, consistent with a large underestimation, by all reconstructions, of the population variance of V(H) (see Table III).

As mentioned before, the $A^1\Pi^+$ state is 2-fold spatially degenerate, and therefore its wave function can be chosen as any linear combination of its constituting states. We have chosen here one in which both states have the same weight. Since the Π states do not have axial symmetry, neither does the ELF.

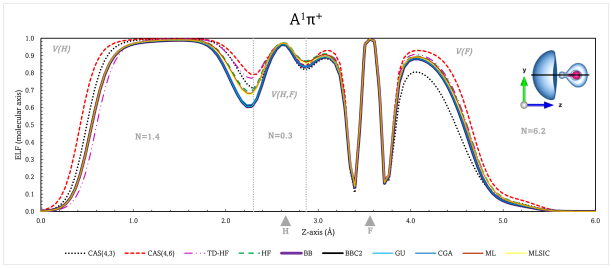

FIG. 2. Profile of the electron localization function (ELF) along the internuclear axis in the first excited state ($A^1\Pi^+$) of the HF molecule as computed with CASSCF and several reconstructions of the 2-PDM at the TD-DFT level (see Table I). The inset shows the line along which the ELF has been plotted as well as an ELF isosurface with an isovalue of 0.87. F and H are depicted as red and light-gray points, respectively. The positions of F and H are marked with light-gray triangles. Vertical dashed lines indicate the location of the separatrices between the basins.

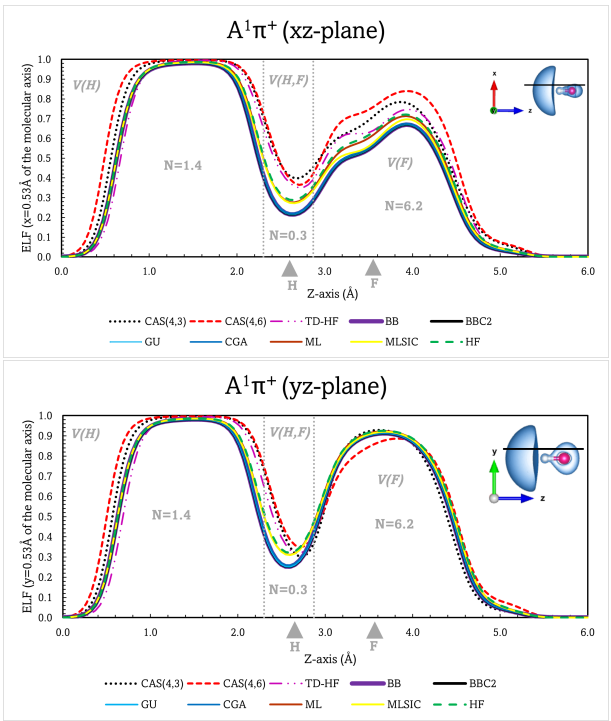

FIG. 3. Profiles of the electron localization function (ELF) computed 1 au (0.53Å) away from the internuclear axis in the first excited state ($A^1\Pi^+$) of the hydrogen fluoride molecule as computed with CASSCF and several reconstructions of the 2 particle-reduced-density-matrix (see Table I). The up/down plots correspond to the ELF in the xz and yz planes, respectively. The insets show the line along which the ELF has been plotted and a ELF= 0.87 isosurface, with F and H being depicted as red and light-gray points. The positions of F and H are marked with light-gray triangles. Vertical dashed lines indicate the location of the separatrices between the basins.

$A^1\Pi^+$ State (FC)										
Basins	CAS(4,3)	CAS(4,6)	TDHF	HF	BB	BBC2	GU	CGA	ML	MLSIC
C(F)	2.0	2.1	2.1	2.1	2.1	2.1	2.1	2.1	2.1	2.1
σ^2	0.39	0.35	0.37	0.37	0.38	0.38	0.38	0.38	0.38	0.38
V(F)	6.6	6.2	6.7	6.7	6.7	6.7	6.7	6.7	6.7	6.7
σ^2	1.82	1.62	0.52	0.52	0.68	0.68	1.11	0.68	1.08	1.15
V(H,F)	0.3	0.3	0.3	0.3	0.3	0.3	0.3	0.3	0.3	0.3
σ^2	0.28	0.28	0.28	0.28	0.27	0.27	0.27	0.27	0.28	0.29
V(H)	1.1	1.4	0.9	0.9	0.9	0.9	0.9	0.9	0.9	0.9
σ^2	0.53	0.49	0.00	0.00	0.25	0.25	0.54	0.25	0.50	0.55
$B^1\Sigma^+$ State (FC)										
Basins	CAS(2,4)		TDHF	HF	BB	BBC2	GU	CGA	ML	MLSIC
C(F)	2.1		2.2	2.2	2.2	2.2	2.2	2.2	2.2	2.2
σ^2	0.37		0.38	0.39	0.39	0.39	0.39	0.39	0.39	0.39
V(F)	6.6		6.8	6.7	6.9	6.9	6.9	6.9	6.9	6.9
σ^2	0.91		0.36	0.48	0.67	0.67	0.99	0.68	1.03	1.07
V(H,F)	0.4		0.2	0.3	0.2	0.2	0.2	0.2	0.2	0.1
σ^2	0.35		0.19	0.26	0.14	0.14	0.14	0.14	0.15	0.13
V(H)	0.8		0.8	0.8	0.8	0.8	0.8	0.8	0.8	0.8
σ^2	0.55		0.04	0.04	0.23	0.23	0.42	0.23	0.49	0.52
$A^1\Sigma^+$ State (Adiabatic)										
Basins	CAS(6,4)	CAS(6,8)	TDHF	HF	BB	BBC2	GU	CGA	ML	MLSIC
C(F)	2.2	2.1	2.2	2.2	2.2	2.2	2.2	2.2	2.2	2.2
σ^2	0.40	0.38	0.37	0.38	0.38	0.38	0.38	0.38	0.38	0.38
V(F)	7.6	7.5	7.3	7.3	7.2	7.2	7.2	7.2	7.2	7.2
σ^2	1.02	0.82	0.15	0.25	0.51	0.51	0.77	0.81	0.81	0.86
V(H)	0.3	0.4	0.6	0.6	0.6	0.5	0.6	0.6	0.6	0.6
σ^2	0.22	0.29	-0.13	-0.05	0.15	0.19	0.34	0.26	0.36	0.43

TABLE III. Population and variance (σ) of the population of the ELF basins of the hydrogen fluoride molecule in the $A^1\Pi^+$ (FC) and $B^1\Sigma^+$ (Franck-Condon and adiabatic) excited states.

With the aim of characterizing this lack of symmetry, we decided to analyze the evolution of the ELF out of the internuclear region, and more specifically by setting a 1 au (0.53 Å) offset with respect to the molecular axis (see Figure 3). The results show that in the yz plane the TD-DFT reconstructions are qualitatively and quantitatively equivalent to the CAS values, whereas in the xz plane, the former significantly underestimate the ELF, especially as far as the V(F) and V(H,F) basins are regarded. Up to this point, it can be concluded that in the $A^1\Pi^+$ state of the HF molecule all 2-PDM approximate TD-DFT reconstructions are equally satisfactory in recovering the correct topology of the ELF. However, from Figures 2 and 3 it is clear that the largest deviations from the CAS references are found for the GU, CGA, BB, and BBC2 functionals.

Besides the straightforward analysis of the ELF values on their own, quite relevant chemical information (aromaticity, reactivity, etc.) can also be extracted from the analysis of basin population statistics. As can be seen from Table III, which summarizes the population and variance of the basins, all approaches underestimate the Rydberg basin population V(H), a result which is transported even more prominently to the variance of the population of the basin, with the exception of the GU, ML and MLSIC functionals. Notably, the HF reconstruction incorrectly predicts that the Rydberg electron is completely uncorrelated from the rest of the molecule, as manifested by the null values of the variance. Since a wavefunction without dynamic correlation, such as TD-HF, yields the same result, it is plausible to attribute this shortcoming of the HF reconstruction to its inability to capture dynamic correlation. These findings are not exclusive to such a basin, but similar results are observed for the fluorine valence basin, albeit showing a population that is close to that of the CASSCF(4,3) result. This indicates that the reconstructions are more effective in capturing the ELF topology than the correlations between electron pairs.

We move now on to the next excited state, $B^1\Sigma^+$, which is usually classified as a $n\sigma_{2p} \rightarrow \sigma^*_{2p}$ single-electron transition. This state is characterized by a moderately large excitation energy of 14.97 eV, according to our CASSCF calculations, which is not far from the experimental values.[72] The TD-DFT and TD-HF results are 15.94 and 14.73 eV, respectively). Indeed, in TD-DFT, the single-electron transition that contributes the most to the excited state is $\sigma_{2p} \rightarrow \sigma^*_{2p}$. $B^1\Sigma^+$ is a bound state to which a strong ionic character is attributed in its equilibrium geometry[73]. Therefore, and for the sake of completeness, here we will study its ELF at both the FC and the equilibrium geometry.

Figs. 4 and 5 summarize our results. At both geometries we appreciate a clear tendency for the RDMFT reconstructions to underestimate the ELF, especially in the valence region of F and in the V(H,F) bond region in the FC geometry, a result which seems rather general to any of the functionals here ex-

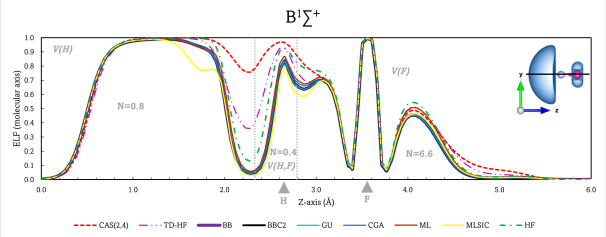

FIG. 4. Profile of the electron localization function (ELF) along the internuclear axis in the Franck-Condon geometry of the second excited state, $B^1\Sigma^+$, of the hydrogen fluoride molecule, as computed with CASSCF and several reconstructions of the 2 particle-reduced-density-matrix (see Table I). The inset shows the line along which the ELF has been plotted and a $ELF = 0.77$ isosurface. F and H are depicted as red and light-gray points in the inset. Positions of F and H are marked with light-gray triangles. Vertical dashed lines indicate the position of the separatrices between the ELF basins.

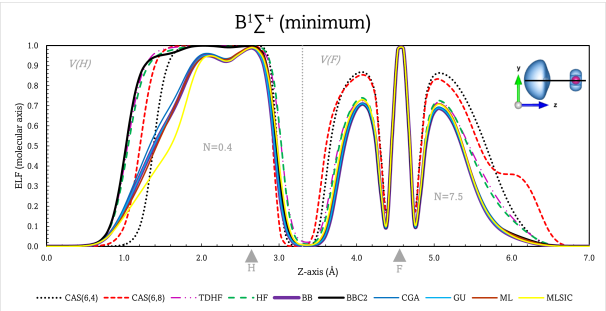

FIG. 5. Profile of the electron localization function (ELF) along the internuclear axis at the equilibrium distance of the second excited state, $B^1\Sigma^+$, of the hydrogen fluoride molecule, as computed with CASSCF and several reconstructions of the 2 particle-reduced-density-matrix (see Table I). The inset shows the line along which the ELF has been plotted and a $ELF = 0.77$ isosurface. F and H are depicted as red and light-gray points in the inset. Positions of F and H are marked with light-gray triangles. Vertical dashed lines indicate the position of the separatrices between the ELF basins.

plored. The non-negligible population (0.4 e) of the V(H,F) basin in the FC geometry suggests that in that state the bond retains its covalency up to a certain extent. Additionally, the appearance of a valence V(H) basin behind the H atoms evidences, once again, the strong Rydberg-like character of such an excitation. Considerably different trends can be found at the equilibrium geometry: there is no V(H,F) bond basin at all and the ELF around the fluorine atom is nearly indistinguishable from that of the free atom. On the other hand, a fraction of an electron (0.4 e) surrounds the nucleus of H. All this points out to a strong increase in the ionic character of the bond upon excitation which agrees with experimental and computational evidence[73].

Finally, when it comes to population fluctuations of the actual ELF basins of the $B^1\Sigma^+$ state, the picture is similar to that found for the $A^1\Pi$ state. From Table III one can draw a general conclusion for Hydrogen Fluoride: TD-DFT reconstructions of the 2-PDM tend to underestimate the variance, becoming less accurate as the fluctuation increases. It can also be concluded that the GU, ML, and MLSIC RDMFTs are those achieving the variances resembling the CASSSF results the most. The reader will also notice that in the case of the equilibrium geometry, the Hartree-Fock reconstruction (both in the TD-DFT and TD-HF cases) leads to non-physical negative variances for the V(H) basin. This negative result can be rationalized in terms of the presence of natural orbitals with small negative occupancy. We think that the HF reconstruction is particularly sensitive to the violation of the sum rule.

B. Polyatomic Molecules

Although the excited states of diatomic molecules present a great diversity/complexity and are very well characterized, routine photochemistry often deals with polyatomic systems. In particular, the first excited state for each given multiplicity is of great interest, since Kasha's rule[77] indicates that it is from this state that most of the radiative deexcitations will likely take place. Taking this into account, we have decided to study the first FC excited of water and benzene. In both cases, the CASSCF excitation energies (7.34 eV for H_2O in its $^1B_1$ state and 5.09 eV for $^1B_{2u}$ benzene) agree reasonably well with experiments and other theoretical estimations[78–84].

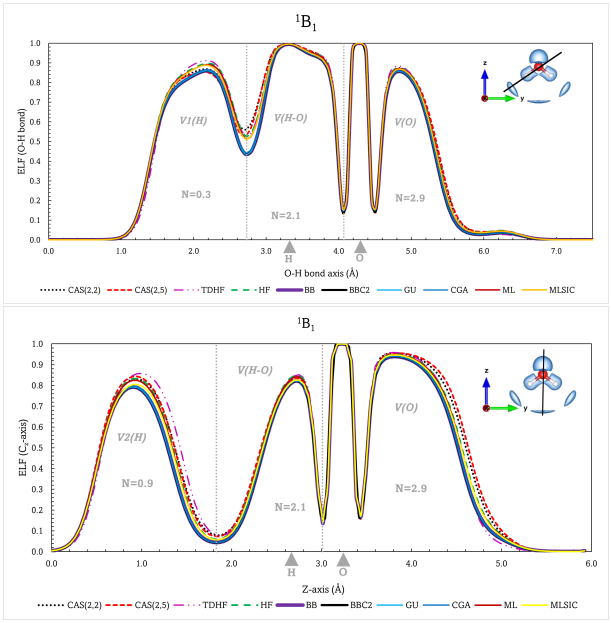

FIG. 6. Profile of the electron localization function (ELF) along the O-H bond axis (up) and in the C_2 axis (down) of the first excited state ($^1B^1$) of the water molecule. The insets show the lines along which the ELF has been plotted and a $ELF = 0.83$ isosurface. O and H are depicted as red and light-gray points in the inset, and with light-gray triangles in the profiles. Vertical dashed lines indicate the position of the separatrices between basins.

Fig. 6 shows the ELF profiles in the Franck-Condon geometry of the first excited state ($^1B_1$) of the water molecule. Apart from the characteristic V(O,H) bond basins and the oxygen non-bonding lone pairs, three valence basins arise in the

$^1B_1$ State (FC)										
Basins	CAS(2,2)	CAS(2,4)	TDHF	HF	BB	BBC2	GU	CGA	ML	MLSIC
C(O)	2.1	2.1	2.1	2.1	2.1	2.1	2.1	2.1	2.1	2.1
σ^2	0.31	0.32	0.32	0.33	0.34	0.33	0.33	0.33	0.33	0.33
V(O)	2.8	2.9	2.8	2.9	2.9	2.9	2.9	2.9	2.9	2.9
σ^2	1.12	1.15	0.90	0.91	1.04	1.04	1.18	1.05	1.17	1.18
V(H,O)	2.1	2.1	2.1	2.1	2.1	2.1	2.1	2.1	2.1	2.1
σ^2	0.90	0.88	0.88	0.87	0.90	0.90	0.92	0.90	0.92	0.92
V1(H)	0.4	0.3	0.4	0.4	0.4	0.4	0.4	0.4	0.4	0.4
σ^2	0.32	0.29	0.23	0.22	0.28	0.28	0.33	0.28	0.33	0.36
V2(H)	0.1	0.2	0.0	0.1	0.1	0.1	0.1	0.1	0.1	0.0
σ^2	0.11	0.18	0.04	0.06	0.05	0.05	0.05	0.05	0.05	0.00

TABLE IV. ELF basin population and variance (σ) for H_2O in its first $^1B_1$ excited state at the Franck-Condon geometry

Basin	CAS(6,6) Ground State	DFT Ground State	CAS(6,6) Excited State	HF	BB BBC2 CGA	GU	ML MLSIC
C(C)	2.1	2.1	2.1	2.1	2.1	2.1	2.1
σ^2	0.25	0.26	0.26	0.26	0.26	0.26	0.26
V(C,H)	2.1	2.1	2.2	2.2	2.2	2.2	2.2
σ^2	0.62	0.65	0.66	0.66	0.68	0.68	0.69
V(C,C)	2.8	2.8	2.7	2.7	2.7	2.7	2.7
σ^2	1.27	1.31	1.29	1.22	1.22	1.23	1.27
Cov[V(C1,C2),V(C2,C3)]	-0.26	-0.27	-0.20	-0.24	-0.24	-0.23	-0.22

TABLE V. ELF basin population, variance (σ) and covariance (between adjacent bond basins) of the benzene molecule in its ground and $^1B_{2u}$ excited states. When results for different reconstructions are numerically equivalent, they are collected in a single column.

nearby vicinity of the H atoms, 2xV(H1) and V(H2). These three basins add up to almost one electron, which corresponds to a Rydberg state[78] of an electron that has left the valence of Oxygen. Furthermore, in this case the topology and statistical properties of the ELF field for all the TD-DFT reconstruction functionals agree well with the multireference calculations. Actually, the main difference between the CAS and TD-DFT results is found in the population (volume) of the V(H2) basin, which has its attractor in the *xz* mirror plane (see Table IV). All of the RDMFT reconstructions as well as the CAS result using a minimum active space underestimate the population and variance of this basin, something which could indicate that it arises from a strong dynamic electron correlation.

We would like to finish our study considering benzene, which is an epitome molecule in the study of how electron localization and aromaticity change upon electronic excitation. In the ground state, the unusual stability exhibited by the C_6H_6 skeleton when compared to other π conjugated systems is often attributed to its aromaticity[85], In a diametrically opposed way, reverse-Hückel[86] and Baird[87] rules classify the first singlet $^1B_{2u}$ excited state (and also the first $^3B_{1u}$ triplet) as antiaromatic[81,87–89]. The ELF of benzene in both states has six equivalent V(C,C) bond basins. In the ground state, the ELF computed at the DFT and CAS(6,6) levels of theory agree very well with one another as far as the topology and statistical properties of the basins are regarded (see Table V). Upon excitation, CAS predicts very small changes in the populations of the V(C,C) and V(C,H) basins, which decrease and increase, respectively. Similarly, the variance of both basins increases only marginally with excitation. From Table V, it becomes clear that all RDMT approximations coincide quite well with the CAS results, both in the population of the basins and in their fluctuations. The only relevant difference is that, with the exception of the ML and MLSIC RDMFTs, TD-DFT results slightly underestimate the variance of the C-C bond basin. Although σ and π separations[90] of the ELF or delocalization index analyses[91,92] are usually better suited to quantify aromaticity changes in general situations, the covariances of the basin populations are sufficient to uncover them in this simple case: a key element of planar aromatic compounds is their ability to delocalize electrons along closed π-bonded paths. That is, the less aromatic an electron state of benzene becomes, the lower the expected electron fluctuation between the V(C,C) basins will be. From the last row of Table V, it is clear that the fluctuation between two neighboring basins is smaller in the excited state than in the ground state. Such a finding would be consistent with a potential decrease in the aromaticity of the skeleton upon excitation, in agreement with chemical intuition and the aforementioned aromaticity rules. Note also that this change in the electron fluctuation is less marked in all DFT reconstructions when compared to the CAS results.

V. CONCLUSIONS

Current state-of-the-art chemical research relies on experimental techniques that allow exquisite spatiotemporal control of the interaction between radiation and matter. The grossest effect of this interaction is the promotion of matter to electronically excited states in which a plethora of photochemical processes might take place. Since chemists think in terms of isolated chemical bonds that form and break, there is no doubt about the importance of having reliable theoretical and computational tools to characterize the chemical bonding in excited states. The ELF has proven to be a reliable tool for this purpose in the ground state. Although it can be calculated for any method in which the 2-PDM is accessible (Eq. 3), such as it is the case for multi-configurational methods of the CASSCF type, the high computational cost associated to these techniques severely limits the complexity of the systems and processes that can be rigorously studied. In this work, we show that fairly reasonable results can be achieved at the computationally feasible TD-DFT level by approximately reconstructing the corresponding 2-PDM under the RDMFT formalism. Given the wide use of TD-DFT in the study of photochemical processes, we have decided to investigate the limits of applicability of this reconstruction strategy. For this purpose, we have used CASSCF as a reference method to assess the accuracy of the ELF when calculated with some of the most commonly employed RDMFT functionals, in prototypical molecules and excited states (HF, H_2O and C_6H_6) covering a diverse range of bonding patterns.

The first important conclusion that can be drawn from this work is that any of the here explored reconstructions of the 2-PDM are quite effective in capturing the right ELF topology. The largest deviations in the latter are found in the case of HF in the $A^1\Pi^+$ and $B^1\Sigma^+$ excited states with the GU, CGA, BB, and BBC2 reconstructions, which are characterized by a strong Rydberg character and the presence of degeneracies (in $A^1\Pi^+$). On the other hand, in the case of H_2O and C_6H_6, all 2-PDM reconstructions recover the topology predicted by CASCCF results. The bond pattern derived from the topology of the ELF agrees with what is accepted for all the states scrutinized: *i)* the $A^1\Pi^+$ states of HF are dissociative with a broken F-H bond and a Rydberg electron; *ii)* the FC geometry of the $B^1\Sigma^+$ state in HF has a strong Rydberg character while the bond becomes strongly ionic at the equilibrium geometry; *iii)* the B_1 state of water is a mixed-valence Rydberg state; and *iv)* the A state of benzene is a valence state of diminished aromaticity. Contrary to the plain ELF topology, correlations between electron pairs, as measured through the variances and covariances of the basin populations, are found to be way more sensitive to the specific form of the RDFMT functionals. All of them tend to underestimate significantly the variance of the basin populations, becoming less accurate as these fluctuations increase. Altogether, the best average performance was found for the ML and MLSIC functionals. The HF reconstruction is particularly sensitive to the loss of the sum rule which could even result in non-physical negative variances. With the evidence presented in this paper we conclude that, in the case of excited states computed with TD-DFT, "robust" reconstructions, such as ML and MLSIC, should be preferred to HF. Note that all the works found in literature[31,34,93,94] that have used the ELF to characterize photochemical processes in excited (spin-preserving) states have used the HF reconstruction proposed by us up to now.[31] Although this is the easiest way to calculate the ELF in an excited state, it may lack the necessary accuracy for non-innocent valence excited states.

ACKNOWLEDGMENTS

This work was partially supported by Fondecyt Grant No. 1220366, by the Center for the Development of Nanoscience and Nanotechnology CEDENNA AFB220001, and by the supercomputing infrastructure of the NLHPC (ECM-02). TG and CC thank to ANID REDES190102. AMP and MG thank the Spanish MICIU, grant PID2021-122763NB-I00 for financial support. MG specifically acknowledges the Spanish MICIU for the predoctoral grant FPU19/02903. We would like to thank Professor Eduard Matito for the fruitful discussion and for the help with the technical details of the source code of the TopMod program.

SUPPORTING INFORMATION

The Supporting information includes details on: *i)*The ELF profiles in the ground state for the hydrogen fluorine molecule; *ii)* The influence of negative occupation numbers on the ELF of HF; *iii)* The ELF isosurfaces for all molecules, excited states, and reconstructions; *iv)* The equilibrium geometries of all molecules; *v)* The molecular orbitals involved in the electronic transitions; and *vi)* a description of the methodology employed to compute the ELF

[1] J. J. Thomson, Lond. Edinb. Dublin Philos. Mag. J. Sci. **44**, 293 (1897).
[2] E. Rutherford, Lond. Edinb. Dublin Philos. Mag. J. Sci. **21**, 669 (1911).
[3] N. Bohr, Nature **121**, 580 (1928).
[4] G. N. Lewis, Journal of the American Chemical Society **38**, 762 (1916).
[5] R. Gillespie and R. S. Nyholm, Quarterly Reviews, Chemical Society **11**, 339 (1957).
[6] R. J. Gillespie and E. A. Robinson, Journal of Computational Chemistry **28**, 87 (2006).
[7] R. Born M.; Oppenheimer, Annalen der Physik **84**, 457 (1927).
[8] P. L. A. Popelier, in *Challenges and Advances in Computational Chemistry and Physics* (Springer International Publishing, Cham, 2016) pp. 23–52.
[9] R. F. W. Bader, Accounts of Chemical Research **18**, 9 (1985).
[10] A. D. Becke and K. E. Edgecombe, The Journal of chemical physics **92**, 5397 (1990).
[11] A. Savin, A. D. Becke, J. Flad, R. Nesper, H. Preuss, and H. G. Vonschnering, Angewandte Chemie **30**, 409 (1991).
[12] A. Savin, O. Jepsen, J. Flad, O. K. Andersen, H. Preuss, and H. G. von Schnering, Angewandte Chemie International Edition in English **31**, 187 (1992).
[13] B. Silvi and A. Savin, Nature **371**, 683 (1994).
[14] A. Savin, B. Silvi, and F. Colonna, Canadian Journal of Chemistry-Revue Canadienne De Chimie **74**, 1088 (1996).
[15] A. Savin, R. Nesper, S. Wengert, and T. F. Fässler, Angeii Chem In Ed Engl **36**, 1808 (1997).
[16] M. Kohout, International Journal of Quantum Chemistry **97**, 651 (2004).
[17] A. Savin, Journal of Physics and Chemistry of Solids **65**, 2025 (2004).
[18] P. W. Ayers, Journal of Chemical Sciences **117**, 441 (2005).

[19] J. Sun, A. Ruzsinszky, and J. P. Perdew, Phys. Rev. Lett. **115**, 036402 (2015).
[20] A. E. Hillers-Bendtsen, F. O. Kjeldal, N. Ree, E. Matito, and K. V. Mikkelsen, Phys. Chem. Chem. Phys. (2022).
[21] R. F. W. Bader, D. Bayles, and G. L. Heard, J. Chem. Phys. **112**, 10095 (2000).
[22] Y.-G. Wang, K. B. Wiberg, and N. H. Werstiuk, J. Phys. Chem. A **111**, 3592–3601 (2007).
[23] P. B. Coto, D. Roca-Sanjuán, L. Serrano-Andrés, A. Martín-Pendás, S. Martí, and J. Andrés, J. Chem. Theory Comput. **5**, 3032–3038 (2009).
[24] R. Chávez-Calvillo and J. Hernández-Trujillo, J. Phys. Chem. A **115**, 13036–13044 (2011).
[25] V. Tognetti and L. Joubert, Chemical Physics Letters **557**, 150 (2013).
[26] J. Jara-Cortés, J. M. Guevara-Vela, A. M. Pendás, and J. Hernández-Trujillo, Journal of Computational Chemistry **38**, 957 (2017).
[27] D. Ferro-Costas, E. Francisco, A. M. Pendás, and R. A. Mosquera, ChemPhysChem **17**, 2666 (2016).
[28] D. Ferro-Costas, A. M. Pendás, L. González, and R. A. Mosquera, Phys. Chem. Chem. Phys. **16**, 9249 (2014).
[29] E. I. Sánchez-Flores, R. Chávez-Calvillo, T. A. Keith, G. Cuevas, T. Rocha-Rinza, and F. Cortés-Guzmán, Journal of Computational Chemistry **35**, 820 (2014).
[30] L. Gutiérrez-Arzaluz, F. Cortés-Guzmán, T. Rocha-Rinza, and J. Peón, Phys. Chem. Chem. Phys. **17**, 31608 (2015).
[31] B. Maulen, A. Echeverri, T. Gómez, P. Fuentealba, and C. Cárdenas, Journal of Chemical Theory and Computation **15**, 5532 (2019).
[32] J. Jara-Cortés, T. Rocha-Rinza, and J. Hernández-Trujillo, Computational and Theoretical Chemistry **1053**, 220 (2015).
[33] L. Gutiérrez-Arzaluz, D. Ramírez-Palma, F. Buitrón-Cabrera, T. Rocha-Rinza, F. Cortés-Guzmán, and J. Peon, Chemical Physics Letters **683**, 425 (2017).
[34] C. Guerra, L. Ayarde-Henriquez, M. D.-N. na, C. Cárdenas, P. Pérez, and E. Chamorro, Phys. Chem. Chem. Phys. **23**, 20598 (2021).
[35] M. N. R. Ashfold, B. Cronin, A. L. Devine, R. N. Dixon, and M. G. D. Nix, Science **312**, 1637 (2006).
[36] S. Axelrod, E. Shakhnovich, and R. Gómez-Bombarelli, Nature Communications **13** (2022).
[37] O. R. Alzueta, M. C. Cuquerella, and M. A. Miranda, The Journal of Organic Chemistry **84**, 13329 (2019).
[38] M. Yang, C. Huo, A. Li, Y. Lei, L. Yu, and C. Zhu, Phys. Chem. Chem. Phys. **19**, 12185 (2017).
[39] P. Zhou and K. Han, Accounts of Chemical Research **51**, 1681 (2018).
[40] J. Laksman, E. P. Månsson, A. Sankari, D. Céolin, M. Gisselbrecht, and S. L. Sorensen, Phys. Chem. Chem. Phys. **15**, 19322 (2013).
[41] M. Pastore, E. Mosconi, F. De Angelis, and M. Grätzel, The Journal of Physical Chemistry C **114**, 7205 (2010).
[42] L. F. V. Ferreira, M. Rosário Freixo, A. R. Garcia, and F. Wilkinson, J. Chem. Soc., Faraday Trans. **88**, 15 (1992).
[43] A. M. Cubillas, S. Unterkofler, T. G. Euser, B. J. M. Etzold, A. C. Jones, P. J. Sadler, P. Wasserscheid, and P. S. Russell, Chem. Soc. Rev. **42**, 8629 (2013).
[44] N. B. McGuinness, H. John, M. K. Kavitha, S. Banerjee, D. D. Dionysiou, and S. C. Pillai, in *Photocatalysis: Applications* (The Royal Society of Chemistry, 2016) pp. 204–235.
[45] J. Yuen-Zhou, W. Xiong, and T. Shegai, J. Chem. Phys. **156**, 030401 (2022).
[46] S. Grimme, Chemistry A European Journal **10**, 3423 (2004).
[47] D. P. Tew, W. Klopper, and T. Helgaker, Journal of Computational Chemistry **28**, 1307 (2007).
[48] J. F. Dobson, The Journal of Chemical Physics **94**, 4328 (1991).
[49] J. F. Dobson, The Journal of Chemical Physics **98**, 8870 (1993).
[50] B. Silvi, The Journal of Physical Chemistry A **107**, 3081 (2003).
[51] E. Matito, B. Silvi, M. Duran, and M. Solà, The Journal of Chemical Physics **125**, 024301 (2006).
[52] A. Echeverri, T. Gómez, E. Luppi, C. Botuha, J. Contreras-Garcia, and C. Cárdenas, Manuscript in preparation (2022).
[53] F. Feixas, E. Matito, M. Duran, M. Solà, and B. Silvi, Journal of Chemical Theory and Computation **6**, 2736 (2010).
[54] R. Parr, *Density-functional theory of atoms and molecules* (Oxford University Press Clarendon Press, New York Oxford England, 1989).
[55] R. McWeeny, *Methods of Molecular Quantum Mechanics* (Academic, London, 1989).
[56] R. McWeeny and B. T. Sutcliffe, *Methods of Molecular Quantum Mechanics*, Monographs of Theoretical Chemistry, Vol. 2 (Academic Press, London, 1969).
[57] T. L. Gilbert, Phys. Rev. B **12**, 2111 (1975).
[58] M. A. Buijse and E. J. Baerends, Molecular Physics **100**, 401 (2002).
[59] M. Buijse and P. P. E. Baerends (1991).
[60] S. Goedecker and C. J. Umrigar, Phys. Rev. Lett. **81**, 866 (1998).
[61] O. Gritsenko, K. Pernal, and E. J. Baerends, The Journal of Chemical Physics **122**, 204102 (2005).
[62] G. Csányi and T. A. Arias, Phys. Rev. B **61**, 7348 (2000).
[63] G. Csányi, S. Goedecker, and T. A. Arias, Physical Review A **65** (2002), 10.1103/physreva.65.032510.
[64] M. A. L. Marques and N. N. Lathiotakis, Physical Review A **77** (2008), 10.1103/physreva.77.032509.
[65] J. D. Chai and M. Head-Gordon, Phys. Chem. Chem. Phys. **10**, 6615 (2008).
[66] F. Weigend and R. Ahlrichs, Phys. Chem. Chem. Phys. **7**, 3297 (2005).
[67] M. J. Frisch, G. W. Trucks, H. B. Schlegel, G. E. Scuseria, M. A. Robb, J. R. Cheeseman, G. Scalmani, V. Barone, B. Mennucci, G. A. Petersson, H. Nakatsuji, M. Caricato, X. Li, H. P. Hratchian, A. F. Izmaylov, J. Bloino, G. Zheng, J. L. Sonnenberg, M. Hada, M. Ehara, K. Toyota, R. Fukuda, J. Hasegawa, M. Ishida, T. Nakajima, Y. Honda, O. Kitao, H. Nakai, T. Vreven, J. A. Montgomery, J. E. Peralta, F. Ogliaro, M. Bearpark, J. J. Heyd, E. Brothers, K. N. Kudin, V. N. Staroverov, R. Kobayashi, J. Normand, K. Raghavachari, A. Rendell, J. C. Burant, S. S. Iyengar, J. Tomasi, M. Cossi, N. Rega, J. M. Millam, M. Klene, J. E. Knox, J. B. Cross, V. Bakken, C. Adamo, J. Jaramillo, R. Gomperts, R. E. Stratmann, O. Yazyev, A. J. Austin, R. Cammi, C. Pomelli, J. W. Ochterski, R. L. Martin, K. Morokuma, V. G. Zakrzewski, G. A. Voth, P. Salvador, J. J. Dannenberg, S. Dapprich, A. D. Daniels, O. Farkas, J. B. Foresman, J. V. Ortiz, J. Cioslowski, and D. J. Fox, "Gaussian 09 revision a.2," (2009).
[68] F. F. S. Noury, X. Krokidis and B. Silvi, "Topmod package," (1997).
[69] M. S. Gordon, M. W. Schmidt, G. M. Chaban, K. R. Glaesemann, W. J. Stevens, and C. Gonzalez, J. Chem. Phys. **110**, 4199 (1999).
[70] N. O. of Data and Informatics, "Nist chemistry webbook, srd 69," (-).
[71] A. Hitchcock and C. Brion, Chemical Physics **61**, 281 (1981).
[72] A. Hitchcock, G. Williams, C. Brion, and P. Langhoff, Chemical Physics **88**, 65 (1984).
[73] G. D. Lonardo and A. E. Douglas, Canadian Journal of Physics **51**, 434 (1973).
[74] J. Pitarch-Ruiz, J. Sánchez-Marín, C. Lavín, A. Velasco, and I. Martín, Chemical Physics Letters **476**, 151 (2009).
[75] T. Novoa, J. Contreras-García, P. Fuentealba, and C. Cárdenas, The Journal of Chemical Physics **150**, 204304 (2019).
[76] H. Edelsbrunner and J. L. Harer, *Computational Topology An introduction* (American Mathematical Society, 2010).
[77] M. Kasha, Discuss. Faraday Soc. **9**, 14 (1950).
[78] M. Rubio, L. Serrano-Andrés, and M. Merchán, The Journal of Chemical Physics **128**, 104305 (2008).
[79] R. Mota, R. Parafita, A. Giuliani, M.-J. H.-F. c, J. L. G. Garcia, S. Hoffmann, N. Mason, P. A. Ribeiro, M. Raposo, and P. L. ao Vieira, Chemical Physics Letters **416**, 152 (2005).
[80] H. t. Wang, W. S. Felps, and S. P. McGlynn, J. Chem. Phys. **67**, 2614 (1977).
[81] P. B. Karadakov, J. Phys. Chem. A **112**, 7303–7309 (2008).
[82] J. Philis, A. Bolovinos, G. Andritsopoulos, E. Pantos, and P. Tsekeris, J. Phys. B: Atom. Mol. Phys. **14**, 3621–3635 (1981).
[83] E. C. da Silva, J. Gerratt, D. L. Cooper, and M. Raimondi, The Journal of Chemical Physics **101**, 3866–3887 (1994).
[84] A. L. SKLAR, Reviews of Modern Physics **14**, 232 (1942).
[85] E. Hückel, Z. physik **70**, 204 (1931).
[86] H. Ottosson, Nature Chemistry **4**, 969 (2012).
[87] N. C. Baird, Journal of the American Chemical Society **94**, 4941 (1972).
[88] T. Slanina, R. Ayub, J. Toldo, J. Sundell, W. Rabten, M. Nicaso, I. Alabugin, I. F. Galván, A. K. Gupta, R. Lindh, A. Orthaber, R. J. Lewis, G. Grönberg, J. Bergman, and H. Ottosson, J. Am. Chem. Soc. **142**, 10942–10954 (2020).
[89] M. Rosenberg, C. Dahlstrand, K. Kilså, and H. Ottosson, Chem. Rev. **114**, 5379–5425 (2014).

[90] J. C. Santos, W. Tiznado, R. Contreras, and P. Fuentealba, The Journal of Chemical Physics **120**, 1670 (2004).
[91] E. Matito, M. Duran, and M. Solá, J. Chem. Phys. **122**, 014109 (2005).
[92] F. Feixas, E. Matito, J. Poater, and M. Solá, Chem. Soc. Rev. **44**, 6434 (2015).
[93] C. Guerra, L. Ayarde-Henríquez, M. D.-N. na, and E. Chamorro, J. Phys. Chem. A **126**, 395 (2022).
[94] C. Guerra, L. Ayarde-Henríquez, M. D.-N. na, and E. Chamorro, ChemPhysChem **22**, 2342 (2021).